



Enhancement of the Chemiluminescence Response of Enzymatic Reactions by Plasmonic Surfaces for Biosensing Applications

Biebele Abel, Babatunde Odukoya, Muzaffer Mohammed, Kadir Aslan✉

Morgan State University, Department of Chemistry, 1700 East Cold Spring Lane, Baltimore, MD 21251 USA

✉ Corresponding author: E-mail: Kadir.Aslan@morgan.edu

Received: Aug. 1, 2015; **Accepted:** Sept. 10, 2015; **Published:** Sept. 15, 2015.

Citation: Biebele Abel, Babatunde Odukoya, Muzaffer Mohammed and Kadir Aslan. Enhancement of the Chemiluminescence Response of Enzymatic Reactions by Plasmonic Surfaces for Biosensing Applications. *Nano Biomed. Eng.* 2015, 7(3), 92-101.

DOI: 10.5101/nbe.v7i3.p92-101.

Abstract

We report the enhancement of chemiluminescence response of horseradish peroxidase (HRP) in bioassays by plasmonic surfaces, which are comprised of (i) silver island films (SIFs) and (ii) metal thin films (silver, gold, copper, and nickel, 1 nm thick) deposited onto glass slides. A model bioassay, based on the interactions of avidin-modified HRP with a monolayer of biotinylated poly(ethylene-glycol)-amine, was employed to evaluate the ability of plasmonic surfaces to enhance chemiluminescence response of HRP. Chemiluminescence response of HRP in model bioassays were increased up to ~3.7-fold as compared to the control samples (i.e. glass slides without plasmonic nanoparticles), where the largest enhancement of the chemiluminescence response was observed on SIFs with high loading. These findings allowed us to demonstrate the use of SIFs (high loading) for the detection of a biologically relevant target protein (glial fibrillary acidic protein or GFAP), where the chemiluminescence response of the standard bioassay for GFAP was enhanced up to ~50% as compared to bioassay on glass slides.

Keywords: Silver island films; Horse radish peroxidase; Glial fibrillary acidic protein; Amplification of chemiluminescence response; Metal-enhanced chemiluminescence; Metal-enhanced fluorescence

Introduction

Chemiluminescence-based detection is routinely employed in a variety of applications, such as clinical diagnosis [1, 2], safety assessment [3], and environmental monitoring [4], due its high sensitivity, wide linear range and cost effectiveness [5]. Chemiluminescence reactions typically require short incubation times in the order of seconds to minutes, which can be terminated on-demand using stopping reagents. However, chemiluminescence-based

detection is also known to have certain shortcomings, such as, poor selectivity and low emission intensity generated by the chemical reactions catalyzed by enzymes in small volumes, which is due to the low efficiency in transforming chemical energy into light [6]. Several strategies were developed to enhance the chemiluminescence emission of chemical reactions catalyzed by enzymes (i.e., enzymatic reactions) [7]. For example, Diaz et al. have demonstrated the use of fluorescein has an enhancer on the chemiluminescence of luminol with horseradish peroxidase (HRP) [8].

These authors proposed that the fluorescent molecules: (i) serve as an enhancer for the chemiluminescence reaction and (ii) promote energy transfer from luminol to fluorescein. However, the chemiluminescence signal enhancement afforded by fluorescein reportedly decreased as the pH of the enzymatic solution increased; due to the decrease in the concentration of protonated fluorescein [8]. Another method used for the enhancement of chemiluminescence response of enzymatic reactions reported in literature is the employment of phenol compounds, which require secondary chemical reactions working in conjunction with HRP [9]. Subsequently, chemiluminescence detection based on enzymatic reactions have also been exploited in the determination of inorganic phosphates [10] and sugars [11].

Recently, plasmon resonant (i.e., plasmonic) nanoparticles, such as gold [12], silver [13] and platinum [14] were also used for the enhancement of chemiluminescence emission, which can be described by a phenomenon called metal-enhanced chemiluminescence (MEC) [15]. In MEC, metal surface plasmons can be excited by chemically induced electronically excited molecules of chemiluminescent species, which can in turn amplify the chemiluminescence emission from the overall system [15]. Two mechanisms are thought to contribute to the enhancement effect of plasmonic nanoparticles: (i) increase in the local electromagnetic field, and (ii) electronic interaction between the plasmons and chemiluminescence species [15]. MEC studies to date employed plasmonic nanoparticles that were deposited on planar surfaces [14], and hereafter called plasmonic surfaces.

In this work, we investigated the use of plasmonic nanoparticles, SIFs (i.e. low, medium, and high loading) [16, 17, 18] and thin films (silver, gold, copper, and nickel, 1 nm thick) for the amplification of chemiluminescence response generated by enzymatic reactions. To investigate the ability of plasmonic surfaces to enhance the chemiluminescence response in bioassays, we initially employed a model bioassay based on biotin-avidin interactions. The immobilization of avidin-conjugated HRP onto plasmonic surfaces was carried out using a biotinylated linker molecule (BEA-5000 Da). We observed a significant increase in HRP chemiluminescence response as the loading of SIFs was increased from low to high. We also observed the largest chemiluminescence response on SIFs with high loading, a ~3.7-fold increase as compared to

the control sample (i.e., blank glass without SIFs). Additionally, chemiluminescence response was also enhanced on gold thin films (~2.7-fold), silver (~2.0-fold), copper (~2.5-fold) and nickel (~2.2-fold) thin films as compared to blank glass slide without plasmonic thin films. These results afforded us to further investigate the use of SIFs (high loading) for detection of GFAP employing commercially available bioassay. To confirm the effect of SIFs (high loading) on the enzymatic chemiluminescence response of the GFAP bioassays, a control surface (blank glass slides without SIFs) was used. We observed that the enzymatic chemiluminescence response of GFAP bioassay can be enhanced up to 50% and the lower detection limit of 10 ng/mL for GFAP can be obtained by using SIFs with high loading.

Materials and Methods

Materials

Streptavidin-peroxidase from *Streptomyces avidinii* (HRP-streptavidin), protein A from *Staphylococcus aureus*, phosphate buffered saline, potassium chloride (KCl), potassium phosphate monobasic (98%), TritonTM X-100 solution, sodium phosphate dibasic heptahydrate ($\text{Na}_2\text{HPO}_4 \cdot 7\text{H}_2\text{O}$) (A.C.S reagent grade), and silane-prep glass slides were all obtained from Sigma-Aldrich. Super signal west pico chemiluminescence substrate was obtained from Thermo Scientific. Biotin-poly(ethylene glycol) amine (BEA) 5000-Da was brought from Laysan Bio, Inc. Human glial fibrillary acidic protein (GFAP) was procured from Abcam® (CA, USA). Monoclonal mouse anti-human glial fibrillary acidic protein, Clone 6F2, was obtained from Dako, North America, Inc. Peroxidase-labeled antibody to mouse IgG, human serum adsorbed, was purchased from KPL, Inc. Sodium phosphate monobasic anhydrous was obtained from Fisher Scientific. Silver, gold, copper, and nickel targets (57 mm diameter × 0.1 mm thick), silicone isolator adhesive (2.0 mm deep and 4.5 mm diameter) were all obtained from Electron Microscopy Sciences (Hatfield, PA). Glass slides (micro slides, thickness: 0.96 to 1.06 mm) used in this work was obtained from Corning Inc. Triethoxysilylbutyraldehyde and 3-Aminopropyltriethoxysilane were bought from Gelest, Inc. All reagents were used as received unless specially described. All aqueous solutions were prepared using deionized water (>18.0 MΩ·cm resistivity at 25 °C) obtained from Millipore Direct Q3

system except stated otherwise.

Preparation of Silver Island Films (SIFs) onto Silane-prep Glass Slides

The different extent of SIFs, i.e., low, medium, and high loading were chemically deposited onto silane-prepared glass slides using Tollen's reagent scheme, which has been previously described [19]. It is important to note that the low, medium, and high loading designation refers to the extent of surface plasmon resonance peak, and used in this study for the sake of clarity. Detailed characterization of SIFs with different loading can be found in one of our previous publications [19].

Deposition of Silver, Gold, Copper, and Nickel Thin Films (1 nm thick) onto Silane-prep Glass Slide

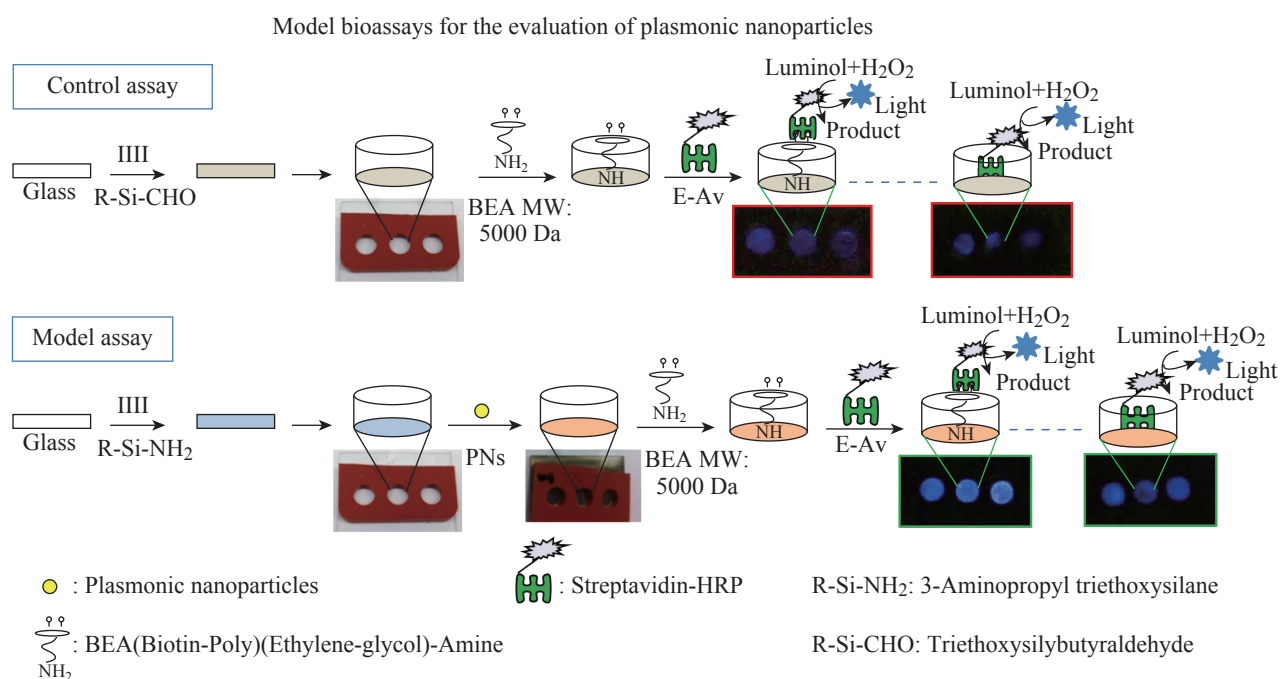
Plasmonic thin films were deposited onto silanized glass slide using a sputter coater (EMS 150R, equipped with film thickness monitor) obtained from Electron Microscopy Science (PA, USA). Specifically, silver, gold, copper, and nickel targets (57 mm diameter x 0.1 mm thick) were used for this investigation. The thickness of plasmonic thin films was adjusted to 1 nm using an inbuilt film thickness monitor.

Surface Modification of Plasmonic Nanoparticles with BEA

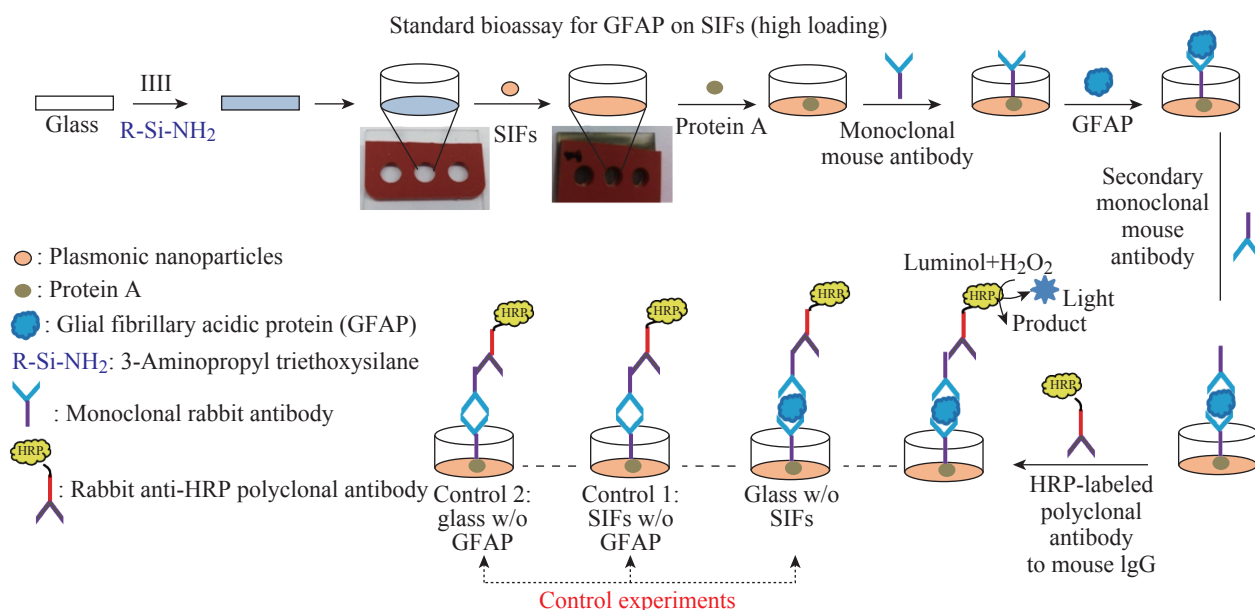
BEA-5000 Da was prepared and attached onto plasmonic surfaces by adopting the procedure from our previous work [20] as shown in Scheme 1. BEA was prepared at a concentration of 0.5 mM using sodium phosphate monobasic buffer solution at pH7. Culture well chambered cover glass was used to cover the plasmonic surfaces and control surface before the addition of 200 μ L of BEA solution in the well chambers, the incubation was kept for 30 minutes. The slides were rinsed with deionized water to remove the unbound BEA.

Surface Modification of Glass Slides with Organosilane (A Control Surface)

The procedure for the surface modification of glass slides using an organosilane was previously described [21]. The modified glass slides were used as our control surface for the immobilization of BEA. [Note: Plasmonic nanoparticles and thin films were omitted on the control experiment. The glass slides were first cleaned in piranha solution (70% sulfuric acid, 30% hydrogen peroxide). The slides were rinsed with deionized water, then kept to dry at room temperature. The cleaned glass slides were later immersed in an



Scheme 1 Schematic depiction of model bioassays carried out on plasmonic surfaces. HRP was deposited to silanized glass, SIFs (low, medium, and high loading), and plasmonic thin films (silver, gold, copper, and nickel) using biotin-avidin interactions. Control experiments include: (i) glass (no plasmonic surfaces), (ii) glass (without plasmonic surfaces and BEA) and (iii) plasmonic surfaces without BEA.



Scheme 2 Schematic depiction of sandwich assay for GFAP on SIFs (high loading): the sandwich assay is based on the deposition of protein A onto SIFs, which supports the binding of monoclonal mouse anti-GFAP antibody. The antibody serves as the capture reagent for binding GFAP at different concentrations (1-100 ng/mL). Subsequently, GFAP bound to the capture antibody is then bound by a secondary antibody. This secondary antibody is then bound by an enzyme-linked antibody (HRP-labeled polyclonal antibody to mouse IgG) which is directed toward itself, but not the capture antibody. The control experiments were carried out on glass slides without SIFs, where GFAP (control 1), SIFs and GFAP (control 2) were omitted from the standard bioassays.

ethanolic solution containing 2% (organosilane) for 1 hour. The organosilane-coated glass slides were rinsed with ethanol and allowed to dry at room temperature.

The sandwich assay was prepared as previously described [22], and the schematic depiction can be seen in Scheme 2.

Preparation of Chemiluminescence Substrate solution

The chemiluminescence substrate for HRP was used as received, which was able to detect low-nanogram amounts of HRP immobilized on the model assay.

Chemiluminescence Assay

The chemiluminescence response of HRP was determined based on the coupled reaction of HRP with luminol to emit blue light. Subsequently, digital images of the emitted light were taken from 0 seconds to 240 seconds in a 5 second interval with a 8 MP digital camera (iPhone from Apple, Inc.). In addition, pixel counts of the digital images were calculated using Adobe Photoshop CS2 software. In the control experiment, where the plasmonic nanoparticles were omitted from the surface, glass slides were used to measure the extent of enzymatic chemiluminescence signal enhancement without the presence of plasmonic nanoparticles and thin films.

Preparation of Sandwich Assay for GFAP on SIFs (high loading)

Results and Discussion

The ability of plasmonic surfaces (nanoparticles and thin films) to enhance chemiluminescence response of HRP were evaluated using a model bioassay. In our model bioassay, a biotinylated target molecule (BEA) was detected on planar surfaces that contain: (i) SIFs (i.e. low, medium, and high loading [17]), and (ii) thin films (i.e., silver, gold, copper, and nickel). In addition, blank glass slides (without plasmonic nanoparticles and thin films) were employed as control surfaces. Subsequently, HRP-streptavidin was immobilized onto the plasmonic and glass surfaces using the biotin-avidin interactions. This process of immobilization afforded for the localization of HRP approximately ~6 nm away from the plasmonic nanoparticles/thin films. The chemiluminescence reagent (i.e. peroxide and luminol, 30 μ L) was then added to the chambers of the silicon isolator containing immobilized HRP to initiate the chemiluminescence reaction. Chemiluminescence emission was quantitatively measured in terms of the total photon counts, which was recorded and compared for 240 seconds. To assess the effects

of plasmonic nanoparticles on the enhancement of chemiluminescence response, several control experiments were also undertaken: (i) model bioassay on blank glass (without plasmonic nanoparticles) and (ii) blank glass without plasmonic nanoparticles and without BEA (Scheme 1).

Chemiluminescence Response from a Model Bioassay on SIFs (low, medium, and high loading)

Figure 1 shows the line plots of chemiluminescence emission intensity (in terms of photon counts) from the model bioassays carried out on SIFs (Fig.1(a)), plasmonic thin films (Fig.1(b)) and control samples (Figs.1(c) and 1(d)) as a function of time. Figure 1(a) shows that the chemiluminescence emission intensity reached a maximum at ~110 seconds on SIFs with low and medium loading as the time progresses from 0 seconds to 240 seconds. On the other hand, the chemiluminescence emission intensity from SIFs with high loading was constant throughout the measurement period. In order to quantify the chemiluminescence

emission and to compare the results of the model bioassay carried out on different surfaces, total photon counts (pixel counts x time) was calculated using the real-color photographs of chemiluminescence emission before and after 240 seconds from the plasmonic surfaces (Table 1- third column). The total photon count detected from SIFs after 240 seconds were determined to be as follows: low loading ($1.75 \pm 0.0011 \times 10^5$), medium loading ($1.84 \pm 0.0035 \times 10^5$), and high loading ($2.76 \pm 0.0035 \times 10^5$) respectively.

These results indicate that the chemiluminescence emission intensity (and total photon count) is increased as the extent of SIFs is increased. As shown previously, SIFs were deposited in a homogeneous manner on glass substrates with size range from 50-90 nm for SIFs with low and medium loading, and ~50 nm for SIFs with high loading [19]. It was also reported that the low and medium loading SIFs appeared as individual nanoparticles as compared to the high loading [19]. Increased chemiluminescence emission is observed from the oxidation of luminol with hydrogen peroxide in the presence of HRP placed ~6 nm away

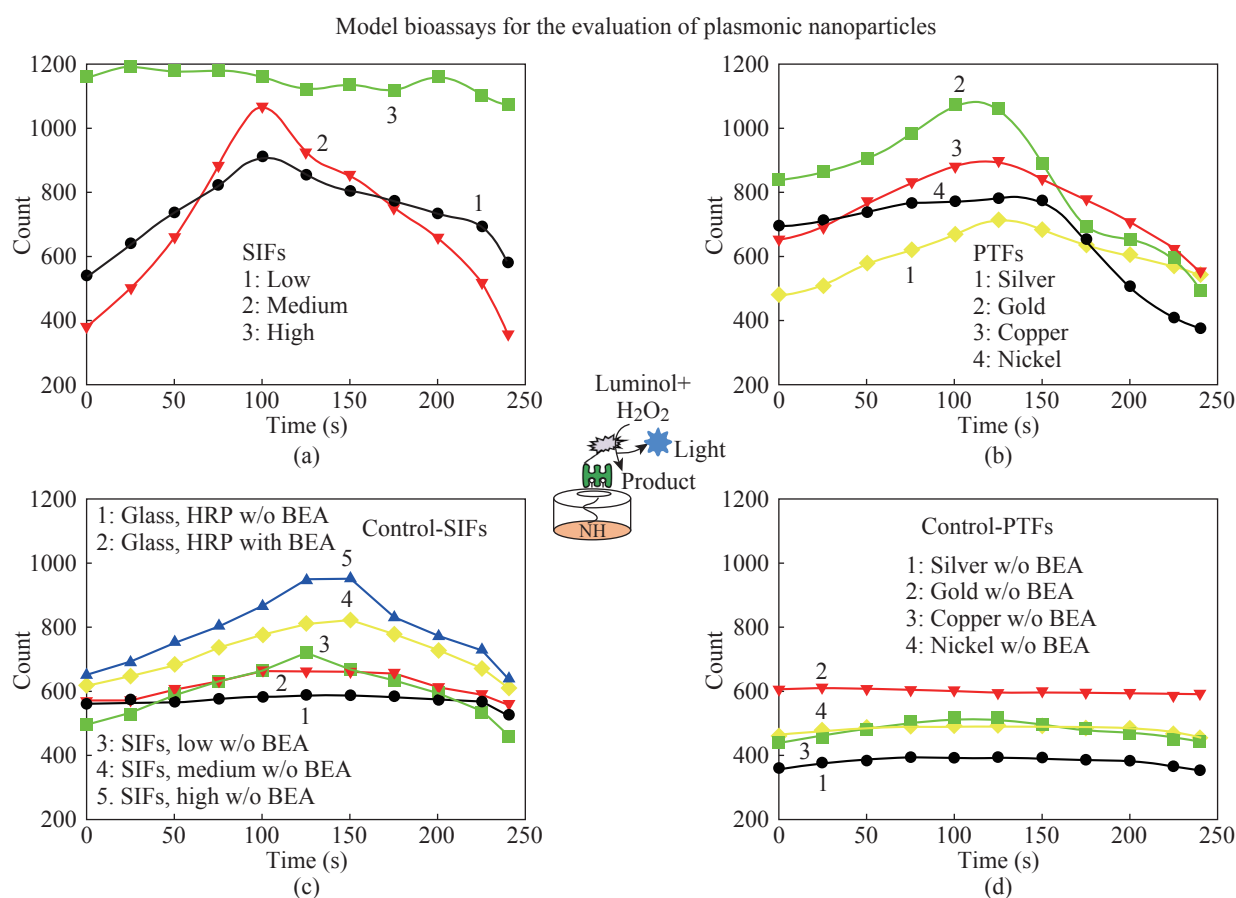

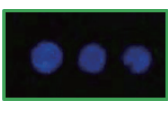

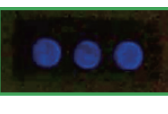

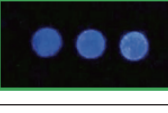
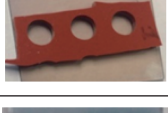
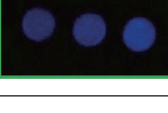
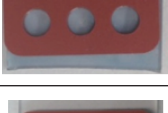

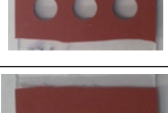
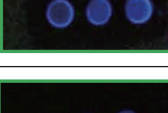
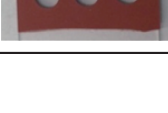
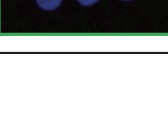


Fig. 1 Chemiluminescence emission intensity as a function of time on (a) SIFs (low, medium, and high loading) and (b) plasmonic thin films (silver, gold, copper, and nickel) and (c and d) corresponding control samples.

Table 1 Summary of results of model bioassays carried out on plasmonic surfaces. Real-color photographs of silver island films, SIFs (low, medium, and high loading) and plasmonic thin films (silver, gold, copper, and nickel) with their respective chemiluminescence images and calculated total photon count (count x sec)

Model bioassay plasmonic thin films (PTF)	Real-Color images of plasmonic nanoparticles	Chemiluminescence images (max. intensity)	Total photon count (count*sec) $\times 10^5$
Low loading (SIFs)			1.75 ± 0.0011
Medium loading (SIFs)			1.84 ± 0.0035
High loading (SIFs)			2.76 ± 0.0035
PTF1: silver (1 nm thick)			1.46 ± 0.0025
PTF2: gold (1 nm thick)			2.02 ± 0.0046
PTF3: copper (1 nm thick)			1.81 ± 0.0022
PTF4: nickel (1 nm thick)			1.63 ± 0.0054

from the surface of SIFs. The observed increase in chemiluminescence emission can be attributed to the close-proximity (<100 nm) interactions of light with surface plasmons of SIFs [15, 23, 24]. The chemically excited states of the chemiluminescent species can couple to surface plasmons, which in turn result in the increase in the chemiluminescence emission intensity [25].

Chemiluminescence Response on Plasmonic Thin Films (1 nm thick silver, gold, copper, and nickel)

Figure 1(b) shows that the chemiluminescence emission intensity measured from different plasmonic thin films reached a maximum value around (110-130 seconds) after the commencement of chemiluminescence reaction, similar to the results obtained from SIFs (low and medium loading). To corroborate these results, the total photon counts

were calculated using the real-color photographs of chemiluminescence emission before and after 240 seconds from the plasmonic thin films: silver ($1.46 \pm 0.0025 \times 10^5$), gold ($2.02 \pm 0.0046 \times 10^5$), copper ($1.81 \pm 0.0022 \times 10^5$), and nickel ($1.63 \pm 0.0054 \times 10^5$) as shown in Table 1. These results imply that thin films of silver, gold, copper, and nickel thin films (1 nm thick) can also be employed for the enhancement of chemiluminescence response using the model bioassay. However, the enhancement of chemiluminescence emission on the plasmonic thin films were lower as compared to SIFs with high loading. This observation can be attributed to the topology of the thin films [26], where the extent of enzymes on the thin films are lower than SIFs [27]. This is because proteins are known to adsorb more on roughened surfaces [28]. It is also important to note that plasmonic thin films thicker than 2 nm did not result in the enhancement of chemiluminescent emission (data not shown), which can be attributed to other coupling effects observed for

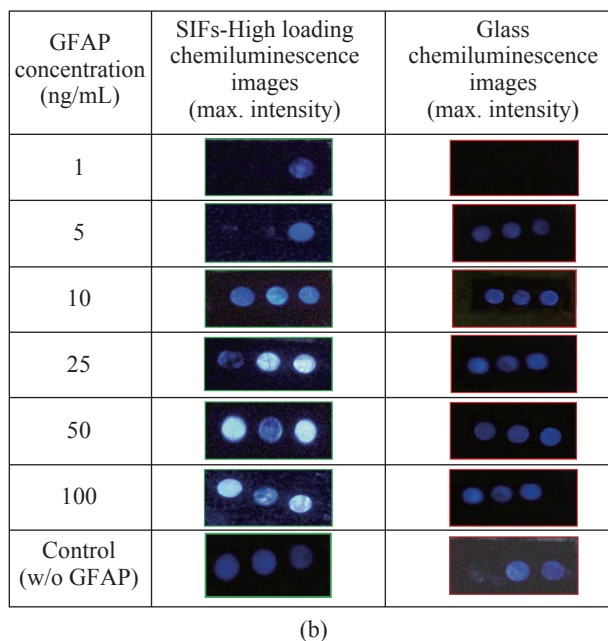
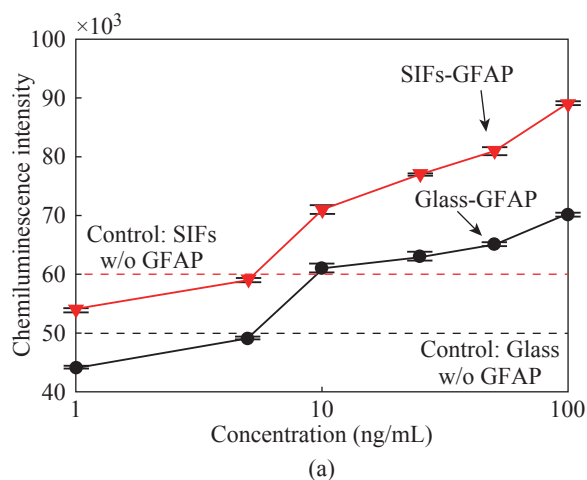


Fig. 2 (a) Total photon count as a function of GFAP at different concentration (1-100 ng/mL) on SIFs (high loading) and glass. (b) Real color photographs of chemiluminescence emission on SIFs (high loading) and glass.

semi-continuous and continuous plasmonic thin films [29, 30, 31, 32].


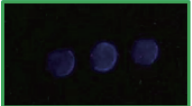
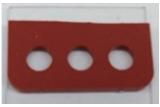
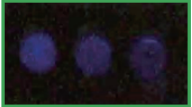











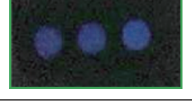
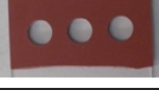
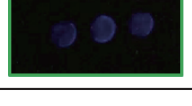
To quantify the effect of SIFs and plasmonic thin films in the enhancement of chemiluminescence response of HRP in the model bioassay, we subsequently employed several control surfaces, where SIFs and plasmonic thin films and / or BEA were omitted from the surfaces, and these results can be seen in Fig.1(c)-1(d). Fig.1(c)-1(d) shows that the chemiluminescence emission as a function of time from control samples are significantly lower than the values observed for SIFs and plasmonic thin films. To corroborate these results, the total photon counts were calculated using the real-color photographs of chemiluminescence emission before and after 240 seconds from the control surfaces, and results can be seen in Table 2. The calculated total photon counts from the control experiments were determined to be as follows: (i) on glass (without SIFs) ($0.74 \pm 0.0018 \times 10^5$), (ii) on glass (without SIFs and without BEA) ($0.68 \pm 0.0022 \times 10^5$), (iii) on SIFs-low (without BEA) ($0.49 \pm 0.0011 \times 10^5$), (iv) on SIFs-medium (without BEA) ($0.84 \pm 0.0013 \times 10^5$), and (v) on SIFs-high (without BEA) ($0.92 \pm 0.0035 \times 10^5$), respectively. Similar results were also obtained when plasmonic thin films were employed without BEA, as shown in Table 2. In addition, the background chemiluminescence emission due to non-specific binding of HRP-avidin on to plasmonic surfaces (no

BEA) were significantly lower than those observed when BEA was present on the surfaces. These results revealed that SIFs with high loading provided the largest enhancement of chemiluminescence response from model bioassays with HRP. The model bioassays run on plasmonic surfaces enabled us to investigate whether SIFs with high loading can also enhance enzymatic chemiluminescence response produced by a commercially available sandwich bioassay for a scientifically relevant target protein, i.e., GFAP.

Detection of GFAP using SIFs (high loading)

GFAP has been used as a protein marker for many brain disorders and diseases, such as Alexander's disease [33, 34, 35]. Scheme 2 depicts a standard sandwich assay for GFAP that was carried out on SIFs with high loading. Several control experiments, where SIFs and GFAP were omitted from the surfaces, were also carried out to assess the effect of SIFs on chemiluminescence response and non-specific detection of GFAP, respectively. The quantification of GFAP on SIFs with high loading was achieved via chemiluminescence measurements and real-color photography. Figure 2(a) shows the plots of the calculated total photon count (labeled as area = intensity x time) detected from the GFAP bioassay at different concentration (1-100 ng/mL) on SIFs (high loading) and glass after 240 seconds. These

Table 2 Summary of results of model bioassays carried out on control surfaces. Real-color photographs of control samples: (i) glass (with BEA and without SIFs), (ii) silanized glass (without SIFs), (iii) SIFs (low, medium, and high loading) without BEA, (iv) Plasmonic thin films (i.e. silver, gold, copper, and nickel without BEA) with their respective chemiluminescence images and total photon count (count x sec)

Model bioassay control samples	Real-Color images of plasmonic nanoparticles	Chemiluminescence images (max. intensity)	Total photon count (count*sec) $\times 10^5$
Glass (w/o SIFs)			0.74 ± 0.0018
Glass (w/o SIFs and BEA)			0.68 ± 0.0022
Low loading (SIFs-w/o BEA)			0.49 ± 0.0011
Medium loading (SIFs-w/o BEA)			0.84 ± 0.0013
High loading (SIFs-w/o BEA)			0.92 ± 0.0035
Silver-1 nm (w/o BEA)			0.45 ± 0.0014
Gold-1 nm (w/o BEA)			0.66 ± 0.0019
Copper-1 nm (w/o BEA)			0.56 ± 0.0018
Nickel-1 nm (w/o BEA)			0.55 ± 0.0019

results revealed an increase in the chemiluminescence response as the concentration of GFAP increases, and also GFAP could be detectable at a minimum concentration of 10 ng/mL.

Moreover, the chemiluminescence response for the identical GFAP bioassay on SIFs with high loading is significantly larger than those observed on blank glass slides, which clearly demonstrates the enhancement of chemiluminescence response by SIFs. The visual evidence for the enhanced chemiluminescence emission was provided with the real-color photographs

of chemiluminescence emission, as shown in Fig.2(b). The chemiluminescence emission (blue color) observed from SIFs (high loading) is significantly higher than those observed from the standard bioassay carried out on glass slides. This observation can be attributed to the coupling interactions between the chemically induced excited states and the surface plasmons of SIFs (reason stated earlier in the text). To determine the background absorbance levels for HRP on all bioassays, several control bioassays were carried out: control 1: SIFs without GFAP, and control 2: glass

without silver and without GFAP. The lower detection limit for GFAP was determined to be 10 ng/mL for standard bioassays on SIFs (high loading) and on glass slides. These results provide direct evidence that chemiluminescence response of biological bioassays can be improved with the incorporation of plasmonic nanostructures. In this regard, our research laboratory is currently working with other biologically relevant target biomolecules, and the results of these studies will be reported in due course.

Conclusions

In this work, we demonstrated the use of plasmonic surfaces, which are comprised of SIFs (low, medium, and high loading), and 1 nm thick thin films (silver, gold, copper, and nickel) for the enhancement of chemiluminescence response of HRP using a model and real-life bioassays. The model bioassay was prepared using a biotinylated linker molecule for the evaluation of plasmonic surfaces. The use of plasmonic surfaces resulted in the enhancement of chemiluminescence response of HRP used in the bioassays. The largest enhancement was observed from SIFs with high loading as compared to other plasmonic surfaces in the model bioassays. These findings suggest that enhanced enzymatic chemiluminescence response for HRP could be achieved by incorporating plasmonic nanoparticles and thin films into current bioassay platforms, such as glass slides. Subsequently, we were able to successfully demonstrate that the incorporation of SIFs (high loading) in to commercially available bioassays for a biologically relevant diagnostic protein (i.e., GFAP) can improve its chemiluminescence response.

Acknowledgement

The project described was supported by Award Number 5-K25EB007565-05 from the National Institute of Biomedical Imaging and Bioengineering. The content is solely the responsibility of the authors and does not necessarily represent the official views of the National Institute of Biomedical Imaging and Bioengineering or the National Institutes of Health.

References

- [1] Q.Y. Zhang, H. Chen, Z. Lin, et al., Comparison of chemiluminescence enzyme immunoassay based on magnetic microparticles with traditional colorimetric

- ELISA for the detection of serum α -fetoprotein, *Journal of Pharmaceutical Analysis*, 2012, 2: 130-135.
- [2] T.B. Xin, S.X. Liang, X. Wang, et al., Determination of estradiol in human serum using magnetic particles-based chemiluminescence immunoassay, *Analytica chimica acta*, 2008, 627: 277-284.
- [3] J.A. Ocaña-González, M. Ramos-Payán, R. Fernández-Torres, et al., Application of chemiluminescence in the analysis of wastewaters-A review. *Talanta*, 2014, 122: 214-222.
- [4] W. Liu, J. Kou, H. Xing, et al., Paper-based chromatographic chemiluminescence chip for the detection of dichlorvos in vegetables, *Biosens Bioelectron*, 2014, 52: 76-81.
- [5] M. Sorouraddin, M. Iranifam, A. Imani-Nabiyi, Determination of penicillin V potassium in pharmaceuticals and spiked human urine by chemiluminescence, *Central European Journal of Chemistry*, 2009, 7: 143-147.
- [6] M. Iranifam, M. Fathinia, T. Sadeghi Rad, et al., A novel selenium nanoparticles-enhanced chemiluminescence system for determination of dinitrobutylphenol, *Talanta*, 2013, 107: 263-269.
- [7] J. Chen, D. Chen, T. Yuan, et al., Microfluidic PCR chips, *Nano Biomed Eng*, 2011, 3: 203-210.
- [8] A.N. Diaz, J.G. Garcia, J. Lovillo, Enhancer effect of fluorescein on the luminol-H₂O₂-horseradish peroxidase chemiluminescence: energy transfer process, *J Biolumin Chemilumin*, 1997, 12: 199-205.
- [9] G. Thorpe, L.J. Kricka, S. Moseley, et al., Phenols as enhancers of the chemiluminescent horseradish peroxidase-luminol-hydrogen peroxide reaction: application in luminescence-monitored enzyme immunoassays, *Clinical chemistry*, 1985, 31: 1335-1341.
- [10] H. Kawasaki, K. Sato, J. Ogawa, et al., Determination of inorganic phosphate by flow injection method with immobilized enzymes and chemiluminescence detection, *Anal Biochem*, 1989, 182: 366-370.
- [11] C.A. Swindlehurst, T.A. Nieman, Flow-injection determination of sugars with immobilized enzyme reactions and chemiluminescence detection, *Analytica Chimica Acta*, 1988, 205: 195-205.
- [12] D. Tian, H. Zhang, Y. Chai, et al., Synthesis of N-(aminobutyl)-N-(ethylisoluminol) functionalized gold nanomaterials for chemiluminescent bio-probe, *Chem Commun (Camb)*, 2011, 47: 4959-4961.
- [13] N. Li, W. Wang, D. Tian, et al., pH-dependent catalytic properties of Pd-Ag nanoparticles in luminol chemiluminescence, *Chem Commun (Camb)*, 2010, 46: 1520-1522.
- [14] C.F. Duan, H. Cui, Time-tunable autocatalytic lucigenin chemiluminescence initiated by platinum nanoparticles and ethanol, *Chem Commun (Camb)*, 2009, 18: 2574-2576.
- [15] K. Aslan, C.D. Geddes, Metal-enhanced chemiluminescence: advanced chemiluminescence concepts for the 21st century, *Chem Soc Rev*, 2009, 38: 2556-2564.
- [16] B. Abel, K. Aslan, Immobilization of enzymes to silver island films for enhanced enzymatic activity, *J Colloid Interface Sci*, 2014, 415: 133-142.
- [17] B. Abel, K. Aslan, Plasmon-Enhanced Enzymatic Reactions 2: Optimization of Enzyme Activity by Surface Modification of Silver Island Films with Biotin-Poly (Ethylene-glycol)-Amine, *Nano Biomed Eng*, 2012, 4: 23-28.
- [18] B. Abel, T. C. Clement, K. Aslan; Enhancement of enzymatic colorimetric response by silver island films on high throughput screening microplates. *J Immunol Methods* 2014, 411: 43-49.

- [19] B. Abel, A. Akinsule, C. Andrews, et al., Plasmon-Enhanced Enzymatic Reactions: A Study of Nanoparticle-Enzyme Distance-and Nanoparticle Loading-Dependent Enzymatic Activity, *Nano biomedicine and engineering*, 2011, 3: 184.
- [20] B. Abel, K. Aslan, Surface modification of plasmonic nanostructured materials with thiolated oligonucleotides in 10 seconds using selective microwave heating, *Ann Phys*, 2012, 524: 741-750.
- [21] A. Carré, W. Birch, V. Lacarrière, Glass Substrates Modified With Organosilanes For DNA Immobilization, in *Silanes and Other Coupling Agents*, Volume 4. 2007.
- [22] J.P. O'callaghan, Quantification of glial fibrillary acidic protein: comparison of slot-immunobinding assays with a novel sandwich ELISA, *Neurotoxicol Teratol*, 1991, 13: 275-281.
- [23] M.H. Chowdhury, K. Aslan, S.N. Malyn, et al., Metal-enhanced chemiluminescence, *Journal of Fluorescence*, 2006, 16: 295-299.
- [24] M.H. Chowdhury, S.N. Malyn, K. Aslan, et al., First Observation of Surface Plasmon-Coupled Chemiluminescence (SPCC), *Chem Phys Lett*, 2007, 435: 114-118.
- [25] K. Aslan, C.D. Geddes, Metal-enhanced chemiluminescence: advanced chemiluminescence concepts for the 21st century, *Chemical Society Reviews*, 2009, 38: 2556-2564.
- [26] A.M. Alabanza, M. Mohammed, K. Aslan, Crystallization of l-alanine in the presence of additives on a circular PMMA platform designed for metal-assisted and microwave-accelerated evaporative crystallization, *CrystEngComm*, 2012, 14: 8424-8431.
- [27] B. Abel, T.S. Kabir, B. Odukoya, et al., Enhancement of Colorimetric Response of Enzymatic Reactions by Thermally Evaporated Plasmonic Thin Films: Application to Glial Fibrillary Acidic Protein, *Anal Methods*, 2015, 7: 1175-1185.
- [28] K. Rechendorff, M.B. Hovgaard, M. Foss, et al., Enhancement of protein adsorption induced by surface roughness, *Langmuir*, 2006, 22: 10885-10888.
- [29] K. Aslan, M. Weisenberg, E. Hortle, et al., Fixed-angle observation of surface plasmon coupled chemiluminescence from palladium thin films, *Applied Physics Letters*, 2009, 95: 123117-123113.
- [30] K. Aslan, M.J.R. Previte, Y. Zhang, et al., Surface plasmon coupled fluorescence in the ultraviolet and visible spectral regions using zinc thin films, *Analytical chemistry*, 2008, 80: 7304-7312.
- [31] K. Aslan, C.D. Geddes, Surface plasmon coupled chemiluminescence from zinc substrates: Directional chemiluminescence, *Applied Physics Letters*, 2009, 94: 073104.
- [32] K. Aslan, C.D. Geddes, Metal-Enhanced Fluorescence: Progress Towards a Unified Plasmon-Fluorophore Description, *Metal-Enhanced Fluorescence*, 2010, 1-23.
- [33] Y. Wada, C. Yanagihara, Y. Nishimura, et al., Familial adult-onset Alexander disease with a novel mutation (D78N) in the glial fibrillary acidic protein gene with unusual bilateral basal ganglia involvement, *J Neurol Sci*, 2013, 331: 161-164.
- [34] A. Messing, Astrocytes and Alexander disease the first, but not last, primary astrocyte disease, in *Physiology and pathophysiology of neuroglia*, in *Henry Stewart Talks: London. p. 1 streaming video file*. 2011.
- [35] P.L. Jany, T.L. Hagemann, A. Messing, GFAP expression as an indicator of disease severity in mouse models of Alexander disease, *ASN Neuro*, 2013, 5: e00109.

Copyright© 2015 Suphanchai Punthawanunt, Biebele Abel, Babatunde Odukoya, Muzaffer Mohammed and Kadir Aslan. This is an open-access article distributed under the terms of the Creative Commons Attribution License, which permits unrestricted use, distribution, and reproduction in any medium, provided the original author and source are credited.